# INTERNATIONAL SOCIETY FOR SOIL MECHANICS AND GEOTECHNICAL ENGINEERING

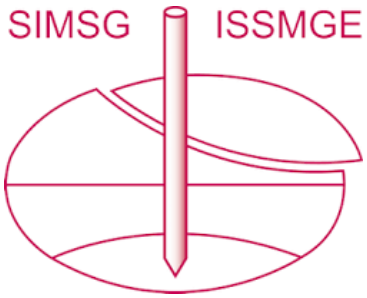


*This paper was downloaded from the Online Library of the International Society for Soil Mechanics and Geotechnical Engineering (ISSMGE). The library is available here:*

*https://www.issmge.org/publications/online-library*

*This is an open-access database that archives thousands of papers published under the Auspices of the ISSMGE and maintained by the Innovation and Development Committee of ISSMGE.*

*The paper was published in the proceedings of the 10th European Conference on Numerical Methods in Geotechnical Engineering and was edited by Lidija Zdravkovic, Stavroula Kontoe, Aikaterini Tsiampousi and David Taborda. The conference was held from June 26th to June 28th 2023 at the Imperial College London, United Kingdom.*

*To see the complete list of papers in the proceedings visit the link below:*

*https://issmge.org/files/NUMGE2023-Preface.pdf*

**Proceedings 10th NUMGE 2023**
10th European Conference on Numerical Methods in Geotechnical Engineering
Zdravkovic L, Kontoe S, Taborda DMG, Tsiampousi A (eds)

© Authors: All rights reserved, 2023
https://doi.org/10.53243/NUMGE2023-216

# Evaluation of continuum modelling approaches for reinforced concrete in geotechnical applications

A.G. Mubarak[1], J.A. Knappett[1], M.J. Brown[1]

[1]*School of Science and Engineering, University of Dundee, Dundee, UK*

**ABSTRACT:** Modelling the structural response of reinforced concrete (RC) elements in geotechnical applications has been implemented using various numerical approaches with different levels of confidence; ranging from simple linear elastic approximations to non-linear section behaviour using embedded beams with moment-curvature ($M$-$\kappa$) relationships within dummy elements. However, the non-linear structural response of continuum RC approaches has not been widely employed in the geotechnical analysis of soil-structure interaction problems. This paper evaluates and compares different combinations of modelling approaches for the concrete and reinforcement, as implemented within the FE code PLAXIS 2D, to simulate the structural response of RC beams using the continuum approach for the concrete with discretely modelled reinforcement. The Concrete Model 'CM' and an equivalent Mohr-Coulomb 'MC' approach are compared for the concrete alongside the use of either embedded plates (with interfaces) or embedded beam rows to efficiently simulate the reinforcement. These approaches are validated against well-documented experimental data of singly and doubly reinforced concrete beams obtained from the literature. The results can be utilised to improve structural precision in Finite Element models in various soil-structure interaction problems (e.g., piles, shallow foundations, retaining walls, tunnel linings) within an integrated geotechnical environment.

**Keywords:** reinforced concrete, Finite Element Method.

## 1 INTRODUCTION

Rigorous analysis of the structural response of the reinforced concrete (RC) elements in soil-structure interaction (SSI) problems is commonly performed using uncoupled structural-geotechnical modelling using specialised FE codes (e.g., ABAQUS or DIANA). While the non-linear structural response can precisely be modelled in such an approach, the geotechnical capabilities of these programs are limited, where simplified assumptions are often required in order to simulate the soil effect via imposing an equivalent active and/or passive subgrade pressure which ignores the non-linear SSI effects.

Accounting for coupled non-linear structural and geotechnical analysis simultaneously in an integrated numerical environment (e.g., PLAXIS FE code) will empower greater precision of results in routine geotechnical analyses and reduce the level of uncertainties associated with simplified assumptions. This paper presents an evaluation of different modelling approaches, implemented within PLAXIS in the plane-strain space, to simulate the structural response of RC elements. The concrete is modelled using a continuum approach with either an equivalent Mohr-Coulomb (MC) or Concrete Model (CM) approach. In addition, two methods were used to model the reinforcing steel bars using either elasto-plastic plates with interface elements or embedded beam elements. The study presents a series of simulations conducted on singly and doubly RC beams under three-point loading tests. Numerical predictions using these modelling approaches were validated against well-documented experimental data from the literature. The endeavour is to develop an approach which can capture the composite behaviour implicitly, avoiding the gross over-simplifications of linear elastic continuum modelling (while remaining similarly efficient) and also avoiding the necessity of generating a moment-curvature relationship *a priori* (avoiding also the decoupling of axial-bending interaction that is inherent in such model).

## 2 MODELLING OF SIMPLY SUPPORTED RC BEAMS IN THE PLAIN-STRAIN SPACE

This section investigates the bending behaviour of simply supported RC beams under three-point loading tests. Two beams were chosen from the literature, a singly reinforced (specimen J-4, Burns and Siess, 1962) and doubly reinforced (specimen A-1, Bresler and Scordelis, 1963) beam, which were constructed using concrete with uniaxial compressive strengths $f'_c$ = 30 and 24 MPa, respectively. Figure 1 shows the experimental setup and the beam cross-sectional details. The following subsections illustrate the procedure followed to model the concrete material as well as the reinforcing bars and confining stirrups using available numerical tools within the commercial FE code PLAXIS (2D).

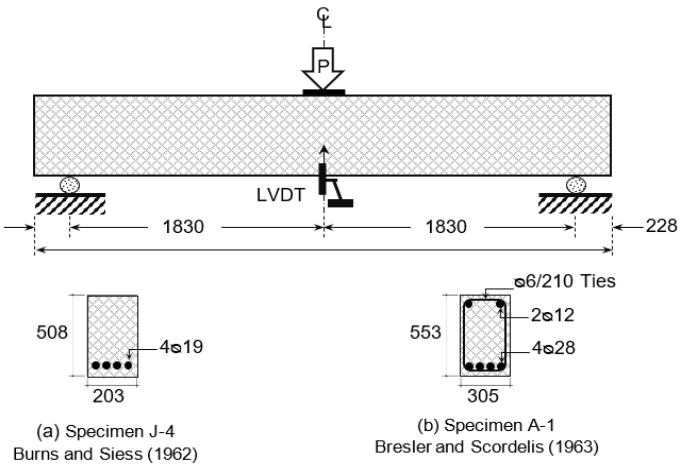


*Figure 1 Geometrical and reinforcement details of the beams under three-point bending: (dimensions in 'mm')*

## 2.1 Constitutive modelling of concrete

Many failure models have been evolved over the years to predict concrete behaviour based on different material behaviour theories, such as elasticity, plasticity, continuum damage and fracture mechanics, or a combination between them. In this study, two constitutive models that are available in PLAXIS materials library were used to model the concrete behaviour, namely the Mohr-Coulomb and the Concrete Model.

According to Mohr-Coulomb (MC), three main parameters are required: equivalent friction angle ($\phi$), equivalent 'apparent' cohesion ($c$) and dilation angle ($\psi$). Vermeer and Borst (1984) reported common friction angles of concrete ranging between 30° to 35°, and dilation angle of around 11°. Equivalent cohesion can be determined by rearranging the Mohr-Coulomb failure envelope principal stress equation in the $\tau-\sigma$ space for an element under uniaxial compression ($\sigma_1 = f_c'$; $\sigma_3 = 0$) as per the following:

$$c = \left(\frac{1-\sin\phi}{2\cos\phi}\right) f_c' \qquad (1)$$

where $f_c'$ is the Unconfined Compressive Strength of concrete (UCS).

The Concrete Model (CM) is an advanced nonlinear, time-dependent constitutive framework to model the behaviour of concrete, which was initially proposed by Schütz *et al.* (2011) to simulate tunnel linings. In this model, the concrete behaviour in compression and tension under multi-axial stress conditions is formulated within the rules of elasto-plasticity. The model can produce the nonlinear plastic strain hardening and softening characteristics of the concrete stress-strain curve. Cracking of concrete is incorporated within a smeared crack model by employing fracture energy principles in compression and tension. The model parameters required to defined the concrete behaviour are: $E_{28} = 4700\sqrt{f_c'}$ ( Young's modulus at 28 days, ACI-318); $\nu$ = 0.2 (Poisson's ratio, reported by Vermeer and Borst, 1984 for concrete); $f_{c,28}$ (Uniaxial compressive strength at 28 days); $f_{t,28}$ (Uniaxial tensile strength, typically taken as $f_t/f_c$ = 0.1); $f_{c0,n}$ (Normalised initially mobilised strength, typically = 0.25); $f_{cf,n}$ (Normalised failure strength, typically = 0.8); $f_{cu,n}$ (Normalised residual strength, typically = 0.1); $f_{tu,n}$ (Ratio of residual to peak tensile strength); $\varepsilon_{cp}^{p} = -0.001$ (typical uniaxial plastic failure strain); $G_{c,28} = 8.8\sqrt{f_c'}$ (Compressive fracture energy, Lertsrisakulrat *et al.* 2001); $G_{t,28} = G_c/250$ (Tensile fracture energy, Nakamura *et al.* 2001); $\phi_{max}$ (Maximum friction angle); $\psi$ (Dilatancy angle). The last two parameters are shared with the MC model. A summary of the constitutive parameters used for the MC and CM concrete modelling approaches is given in Table 1.

*Table 1 Summary of the constitutive parameters selected for MC and CM modelling approaches*

| Mohr-Coulomb | | | |
|---|---|---|---|
| **Parameters** | **Value (J-4)** | **Value (A-1)** | **Unit** |
| $c$ | 7.8 | 6.3 | MPa |
| $\phi$ | 35 | 35 | ° |
| $\psi$ | 11 | 11 | ° |
| **Concrete Model** | | | |
| $E_{28}$ | 25 | 23 | GPa |
| $\nu$ | 0.2 | 0.2 | - |
| $f_{c,28}$ | 30 | 24 | MPa |
| $f_{t,28}$ | 2.4 | 2 | MPa |
| $f_{c0,n}$ | 0.25 | 0.25 | - |
| $f_{cf,n}$ | 0.8 | 0.8 | - |
| $f_{cu,n}$ | 0.1 | 0.1 | - |
| $f_{tu,n}$ | 0 | 0 | - |
| $\varepsilon_{cp}^{p}$ | $-1 \times 10^{-3}$ | $-1 \times 10^{-3}$ | - |
| $G_{c,28}$ | 70 | 50 | kN/m |
| $G_{t,28}$ | 0.2 | 0.15 | kN/m |
| $\phi_{max}$ | 35 | 35 | ° |
| $\psi$ | 11 | 11 | ° |

## 2.2 Idealised stress-strain behaviour of confined and unconfined concrete

It is well established that concrete possesses nonlinear stress-strain behaviour under uniaxial-compression. Various analytical solutions were proposed in the literature to predict such behaviour (e.g., Lim and Ozbakkaloglu, 2014, Mander *et al.* 1988). These analytical models can be used as a benchmark to calibrate the numerical constitutive parameters to fit the uniaxial nonlinear behaviour. Lim and Ozbakkaloglu (2014) proposed an analytical model applicable to both confined and unconfined concrete, and for normal to high-strength concrete classes. Figure 2 shows an example of the stress-

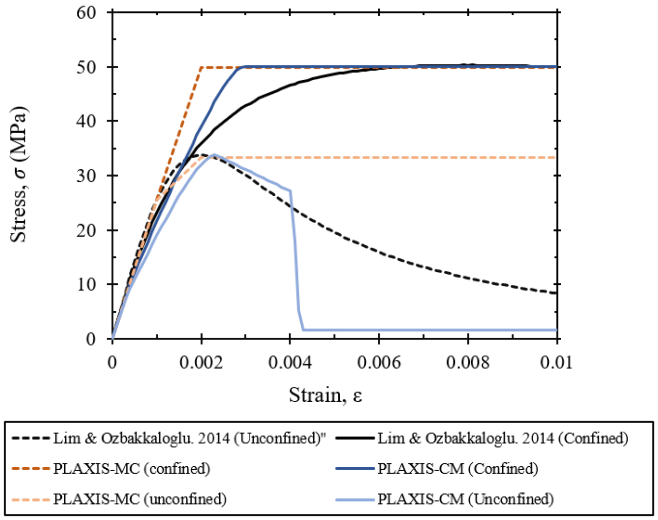


*Figure 2 Idealised stress-strain models for confined and unconfined concrete against MC & CM test fittings*

strain curves for confined and unconfined concrete with compressive strength $f'_c$ = 30 MPa, plotted against MC & CM responses using the parameters in Table 1. The confined response was obtained under triaxial loading conditions with a confining pressure ($\sigma'_3$ = 6.4 MPa) estimated using the suggested procedure by Mander *et al.* (1988) for rectangular sections. Nevertheless, for members under flexure without significant axial load, the effect of confinement provided by the beam stirrups is expected to be small (Park and Paulay, 1975).

### *2.3 Finite Element modelling*

The FE model of the beam setup is shown in Figure 3. The end supports were modelled using a prescribed point displacement with pin and roller restraint properties at each end respectively. A transition element with elastic properties similar to the beam concrete was introduced at the end supports to avoid stress concentrations near the point restraints which might terminate the calculation before the actual beam failure. The model boundary conditions were set such that they were compatible with the constraints in the test setup as illustrated in Figure 3.

The FE model domain for J-4 and A-1 specimens was discretised to a total number of 1160 and 915 triangular plane-strain elements, which corresponds to (2447 nodes) and (1966 nodes) respectively. 6-noded elements were selected, which were found to be precise enough for such applications and which reduce the computational cost.

Elasto-plastic plate elements were initially chosen to model the tension steel in specimen (J-4) and the tension and compression steel in specimen (A-1). Plates had normal (*EA*) and bending (*EI*) stiffness properties per metre length which were used to idealise the fundamental behaviour of steel bars at a given spacing. The plates were assumed to have a bending capacity equal to the yield moment capacity (i.e., $M_{ult} = M_y = n.Z.f_y$, where $Z$ is plastic section modulus and $n$ is the number of bars). Positive and negative interfaces were used between the plate and concrete, to capture potential gapping (normal tensile limit = $R_{inter}.f_t$ = 0.36 MPa) and bar slippage mechanisms (strength and stiffness reduction factor $R_{inter}$ smeared in the interface material to degrade the bond condition).

Alternatively, embedded beam elements at the reinforcement spacing with equivalent elastic stiffness properties were used to model the bond-slip behaviour via limiting skin friction ($\tau_{skin}$). Shear stirrups were modelled using node-to-node (NtN) anchors with axial properties per metre length equivalent to those of the beams. The steel properties for both approaches are summarised in Table 2.

## 3 VALIDATION OF THE NUMERICAL MODELS AGAINST THE TEST RESULTS

In these simulations, various combinations were tested for MC *vs*. CM. Figure 4(a) (b) and (c) (d) show the FE load-displacement response for singly and doubly-reinforced beams (J-4 and A-1) against the experimental data. In these simulations, two main variables affecting the flexural behaviour of the beam were considered, these being the concrete tensile strength (with $f_t$ = 0.7, 1.2 and 2.4 MPa), such that $f_t/f_c \leq 0.1$, and the interface strength between the concrete and plate(s) such that $R_{inter}$ =1 represents a rigid interface (with strength equal to the surrounding concrete).

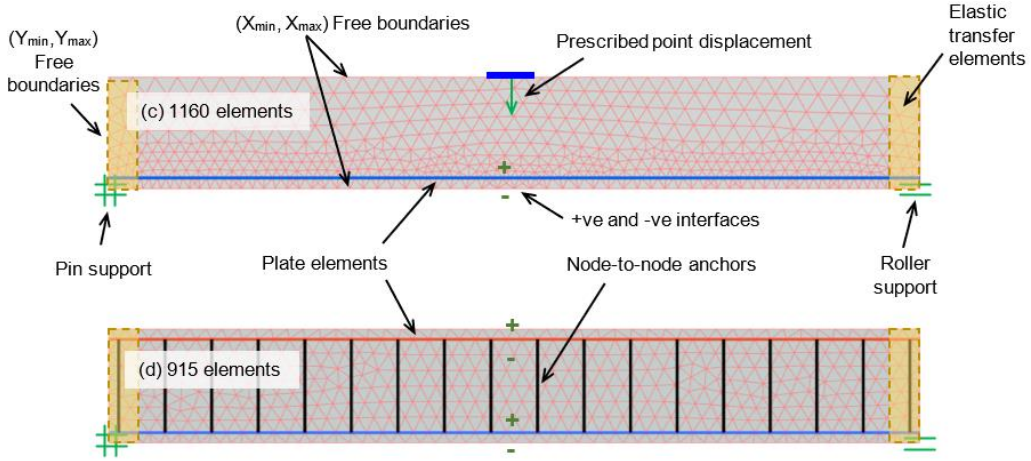


*Figure 3 Plane-strain FE model with the modelling elements identified for (a) singly-reinforced and (b) doubly-reinforced beams*

*Table 2 Steel properties used in singly and doubly RC beam specimens*

| Steel property | Specimen J-4 | Specimen A-1 | | |
|---|---|---|---|---|
| | Bottom Steel | Top Steel | Bottom Steel | Stirrups |
| Material behaviour | Elastoplastic | Elastoplastic | Elastoplastic | Elastoplastic |
| Structural element | Plate | Plate | Plate | NtN Anchor |
| $E_s$ (GPa) | 203 | 200 | 217 | 189 |
| $f_y$ (MPa) | 310 | 345 | 555 | 325 |
| $EA$ (kN/m) | $1.02 \times 10^6$ | $0.167 \times 10^6$ | $1.88 \times 10^6$ | $0.04 \times 10^6$ |
| $EI$ (kN.m$^2$/m) | 12.45 | 1.68 | 99.2 | - |
| $N_p$ (kN/m) | 1556 | 287 | 2945 | 68 |
| $R_{inter}$ (-) † | 0.15 | 0.15 | 0.15 | - |

† $R_{inter}$ is the interface strength parameter

The results show that MC generally over-predicts the load capacity of the beam at typical tensile strength values (i.e., 2.4 MPa, $f_t/f_c = 0.1$), and manifests a stiffer deformational response after the first-yield point (e.g., >50 kN in Figure 4(a) and (b) and >200 kN in Figure 4(c) and (d). Such behaviour was improved by reducing the concrete tensile strength to 1.2 MPa and 0.7 MPa respectively, where the latter results in a good prediction for the beam capacity and stiffness with error percentage of 10% (Figure 4(a) and (c)).

The CM appears to demonstrate a slightly stiffer response at typical tensile strengths ($f_t$ = 2.4MPa), which was improved at lower values ($f_t$ =1.2 MPa, 0.7 MPa). However, the capacity appears not to be affected significantly by the tensile strength in this approach.

The effect of uncertainty in the steel-concrete bond condition was also explored by allowing some bond-slip to take place by decreasing the strength and stiffness of the interface ($R_{inter}$ < 1) as shown in Figure 4(b) and (d). This allows better fitting to the experimental data after the first-yield to the peak capacity, particularly for CM. Reduction of this parameter may yield poor results in CM if larger limitations on load transfer are modelled (e.g., $R_{inter}$ < 0.1).

Figure 5(a-d) shows the load-displacement response of the RC beams (J-4, A-1), using the MC and CM approaches with steel rebars modelled as embedded beams (EB) and compared to the responses utilising plate elements and interfaces (PLATE).

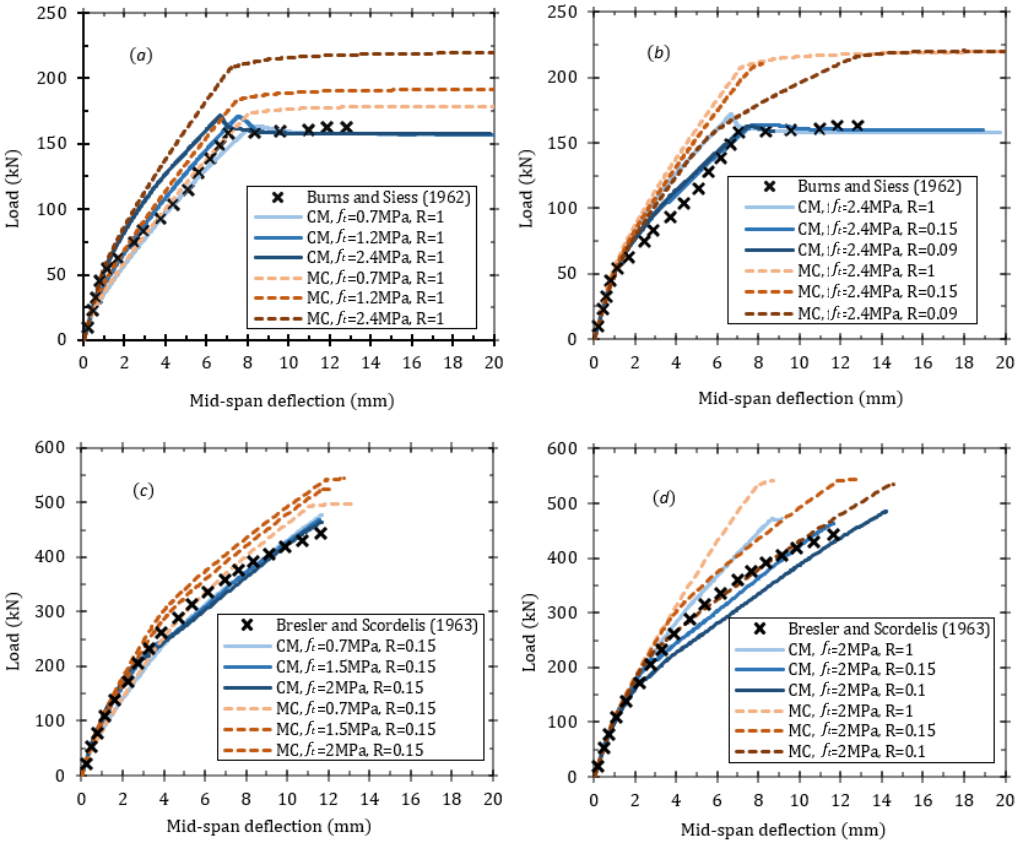


*Figure 4. FE verification of the load-displacement response of experimental beams loaded in bending using Mohr-Coulomb and Concrete models for concrete, for varying $f_t$ and $R_{inter}$ values. (a) and (b) singly-reinforced 'specimen J-4, (c) and (d) doubly-reinforced beam*

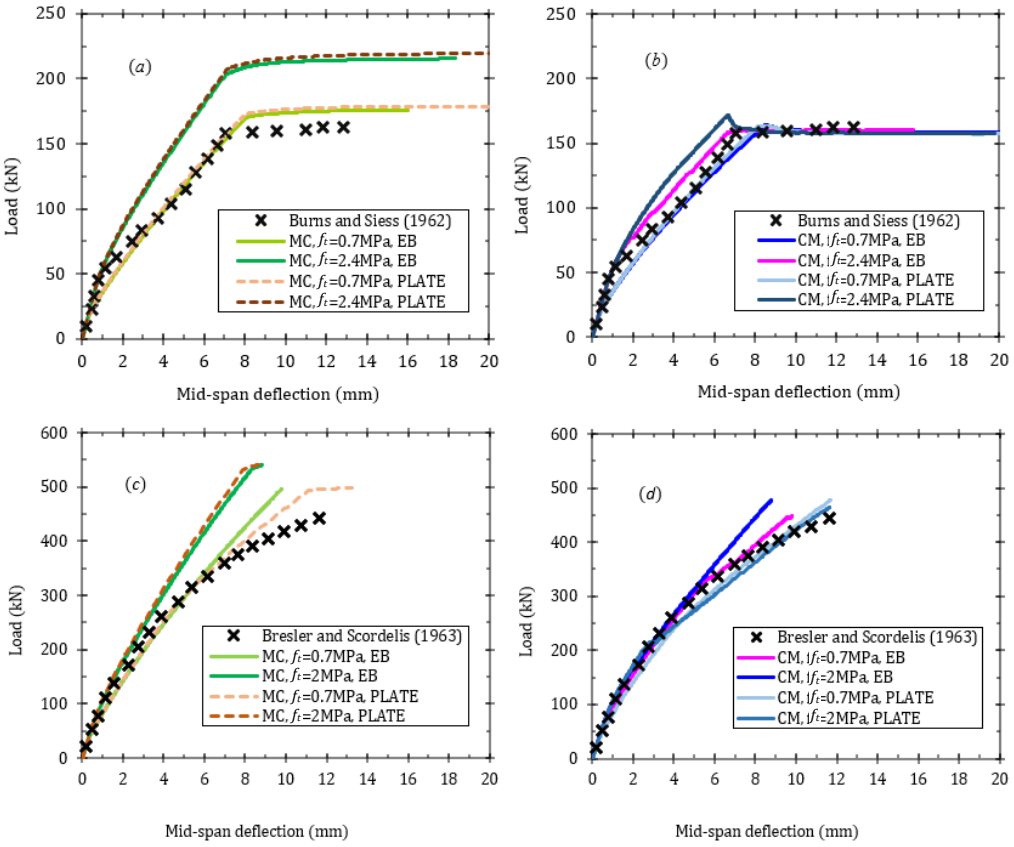


*Figure 5 Load-displacement response with longitudinal steel modelled as embedded beams and compared with the plate elements response; where (a) MC/singly RC 'J-4', (b) CM/singly RC 'J-4', (c) MC/doubly RC 'A-1', (d) CM/doubly RC 'A-1'*

The embedded beam elements have equivalent stiffness and strength parameters to those in Table 2, with a pull-out resistance $\tau_{skin,\,max}$ = 1250 kN/m and 1940 kN/m for J-4 and A-1, respectively, which were estimated according to Eligehausen *et al.* (1982) to model the bars' slippage. The results show that embedded beam elements did not manifest a significant difference as compared to the responses of beams modelled with plate elements. In both cases, the behaviour remained affected by the concrete tensile strength (although this is a property related to MC and CM and not to the embedded elements). The plate cases shown in Figure 5 had a rigid interface strength (i.e., $R_{inter}$ = 1), and since the embedded elements had a skin friction much higher than the yield strength of steel ($\tau_{skin,\,max} > N_p/A_{surface}$), they resulted in near-identical response curves.

To investigate the reason why MC tended to over-estimate load capacity and stiffness beyond the first-yield point, a group of FE triaxial compressive strength test simulations with different confinement levels were generated, as shown in Figure 6. The MC and CM failure envelopes in the shear-normal stress ($\tau$–$\sigma_n$) space were drawn using Mohr-circles representing the peak principal stress condition that corresponds to the peak capacity in the load-displacement response (Figure 2). The linear MC envelope with tension cut-off over-estimates the shear strength capacity in compression and tension compared with the nonlinear CM envelope.

The plastic softening behaviour that characterises the compressive behaviour in CM is furthermore not captured by the perfect plasticity assumption in MC (see Figure 2). In the same manner, the tensile strength of concrete degrades to zero in the CM while the strength is maintained in MC.

Figure 7 shows shear-strain ($\gamma_s$) contours using the MC and CM for the singly- and doubly-reinforced beams compared against the observed experimental crack patterns (overlying darker lines). In general, strain localisation zones at the bottom of the beam show more realistic patterns in CM simulations compared to a bulb-like strain concentration in MC.

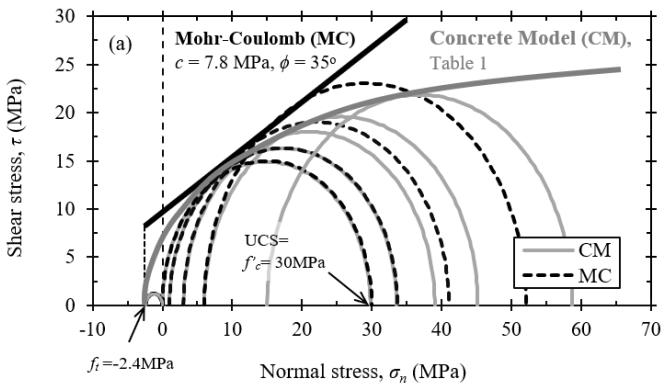


*Figure 6 Comparison between the MC and CM failure envelopes in the $\tau$-$\sigma$ space using simulated FE compressive triaxial concrete tests with different confining pressures*

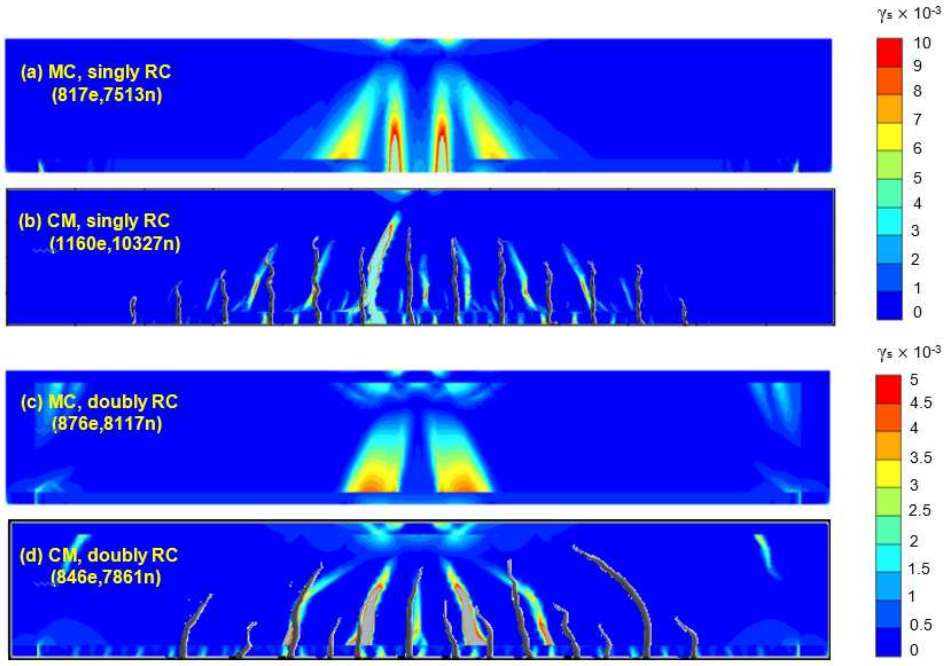


*Figure 5 Shear-strain ($\gamma_s$) distributions for singly (a & c) and doubly (b & d) RC specimens using CM and CM approaches. **N.B**. **e** and **n** represent the number of FE mesh elements and nodes respectively.*

## 4 CONCLUSIONS

In light of the numerical results from various modelling approaches to model RC beams (flexural members), the following key findings can be drawn:

1. MC criterion can be used as a first-order approximation approach to model simple RC structures. However, it tends to over-predict the capacity of the concrete component at typical tensile strength values ($f_t/f_c \leq 0.1$). This can be addressed by artificially lowering the tensile strength to residual values ($f_t \leq$ 1MPa) to represent a cracked section.
2. CM offers a more sophisticated technique to model RC behaviour with confidence and higher accuracy (usually with precision around ±5%). The model is reliable for the range of RC configurations under flexural loading considered herein.
3. Different reinforcement modelling methods can be employed to model the reinforcing steel, either using elasto-plastic plate elements (PL) with interfaces, or by the embedded beams (EB) which have implicit frictional interfaces. Both methods demonstrated similar results approximately.
4. In the case of plates, setting the value of the interface stiffness parameter $R_{inter}$ is paramount to control the stiffness of the load-deformation response after the first-yield point. According to the investigated beams, a suitable parameter in the range of ($0.1 \leq R_{inter} \leq 0.15$) appears to be adequate to simulate the load-transfer between concrete and reinforcement. This is equivalent to the pull-out resistance in EBs.

Having said that, the presented modelling approaches offer a useful tool to model the RC elements necessary for geotechnical applications (e.g., tunnel linings, foundations etc.) at working and ultimate loads scenarios (i.e., Serviceability and Ultimate Limit States, 'SLS', ULS' respectively).

## 5 REFERENCES

Bresler, B., Scordelis, A.C. 1963. "Shear Strength of Reinforced Concrete Beams". Journal of ACI, Vol. 60, No. 1, pp.92-100.

Burns, N.H., Siess, C.P. 1962. "Load-Deformation Characteristics of Beam-Column Connections in Reinforced Concrete". Civil Engineering Studies, SRS No. 234, University of Illinois, Urbana.

Eligehausen R., Popov, E. P., Bertero V. V. 1983. ''Local bondstress-slip relationships of deformed bars under generalized excita-tions.''Rep. No. UCB/EERC 83-23, Univ. of California, Berkeley,Calif

Lim, J.C., Ozbakkaloglu, T. 2014. Stress–strain model for normal-and light-weight concretes under uniaxial and triaxial compression. Construction and Building Materials, 71, pp.492-509.

Mander, J. B., Priestley, M. J. N., Park, R. 1988. Theoretical stress-strain model for confined concrete. J. Struct. Engrg., ASCE, 114-8-, 1804-1826.

Park, R., Paulay, T. 1975. Reinforced Concrete Structures. Christchurch: John Wiley & Sons, Inc.

Schütz, R., Potts, D., Zdravkovic, L. 2011. Advanced constitutive modelling of shotcrete: Model formulation and calibration. Computers and Geotechnics, 38(6), pp.834-845.

Vermeer, P.A., de Borst 1984. Non-associated plasticity for soils, concrete and rocks. In: Heron (Ed.), Stevin-Laboratory of Civil Engineering, vol. 29(3à). University of Technology, Delft Institute TNO for Building Materials and Building Structures, Rijswijk, The Netherlands, pp.170-174.